Analysis for the Catalytic Ignition of Methane in a Stagnation-Point Flow

C. Treviño
Facultad de Ciencias, UNAM, 04510 México D.F., México

The catalytic ignition of a mixture of methane and air in a planar stagnation-point flow over a platinum foil is studied. The heterogeneous reaction mechanism is modeled with twelve heterogeneous reactions, including the adsorption processes of both reactants, the desorption kinetics of reactants and main products, and a set of surface reactions of the Hinshelwood− Langmuir type. The critical conditions for the catalytic ignition are found using high activation energy asymptotics of the desorption kinetics of the adsorbed reactant O(s). The analytical results are compared with published experimental data. The agreement is good, at least qualitatively.

Introduction

The catalytic ignition of fuel/air mixtures has received considerable attention in the literature in the past few years, due to its role in the startup in the automobile catalytic converters, catalytic, and the catalytically assisted combustors (Pfefferle and Pfefferle, 1987; Rinmeno et al., 1993; Fassihi et al., 1993; Deutschmann et al., 1996; Veser and Schmidt, 1996; Bui et al., 1997a). Experimental and theoretical studies of catalytic ignition have been published, increasing our knowledge about several aspects related to this type of critical nonlinear process. Schmidt and coworkers (Williams et al., 1991; Veser and Schmidt, 1996) presented experimental results of the catalytic ignition of different hydrocarbons on platinum using a stagnation-point flow configuration. They showed that for methane, the critical ignition temperature decreases as the mixtures become richer. The ignition process has been studied from the theoretical point of view, by either numerical simulations using elementary chemistry (Song et al., 1990; Warnatz, 1992; Warnatz et al., 1994; Deutschmann et al., 1996; Bui et al., 1996, 1997a,b), or by large activation energy asymptotic analyses using a one-step overall reaction mechanism (Treviño and Fernández-Pello, 1981; Treviño, 1983; Treviño and Peters, 1985; Treviño and Méndez, 1996). The basic principles of heterogeneous catalysis have been described elsewhere (Ertl, 1982; Williams et al., 1992). Williams et al. (1992) presented for the first time a model for the catalytic combustion of hydrogen at high temperatures. They presented the rate parameters of a detailed surface chemistry. In a series of papers, Warnatz and coworkers (Warnatz, 1992; Warnatz et al., 1994) and Bui et al. (1997c) studied the catalytic combustion and ignition of hydrogen using detailed kinetic mechanisms for both surface and gas-phase reactions. Warnatz et al. (1994) compared their results with previously reported data of Ljungström et al. (1989). Deutschmann et al. (1996) studied the catalytic ignition of different fuels on different catalyst materials. They indicated that the ignition process is an abrupt transition from a kinetically controlled system to one controlled by mass transport, and that it depends mainly on the adsorption−desorption reaction steps. In their numerical simulations they showed that one or the other reactants almost covered the surface prior to ignition. Behrendt et al. (1996) and Bui et al. (1997b) reported numerical calculations for methane and air that compared well with experimental results. There is a need to obtain reduced kinetic schemes for the catalytic combustion that help to build a bridge between the full numerical works and the theories developed using an overall one-step reaction for the surface kinetics. In an earlier work, Treviño (1998) presented an asymptotic analysis of the catalytic ignition using a simplified model for the heterogeneous chemistry with the adsorption−desorption reactions of both reactants, one surface reaction, and the desorption of the main product. The critical conditions for ignition have been derived and, in a closed form, the parametric influence on this critical process obtained. The relationship between this simplified kinetic model and a one-step surface reaction has been obtained.

The objective of this work is to extend the previous analysis (Treviño, 1998) to apply to the case of the heterogeneous ignition of methane on a platinum catalyst, using the stagnation-point flow configuration, and to compare it with the experimental data reported by Veser and Schmidt (1996).

Formulation

Gas-phase governing equations

The physical model under study is shown in Figure 1. A premixed combustible mixture of methane and air, with mass concentrations denoted by $\overline{Y}_{CH_4\infty}$ and $\overline{Y}_{O_2\infty}$, flows with a velocity gradient a and temperature T_∞, perpendicular to a platinum plate of finite thickness h. The lower surface of the plate is kept to the same temperature T_∞. Due to the exothermic heterogeneous reactions, the temperature at the catalyst will rise, reaching the asymptotic value obtained from the balance of the reaction heat and the heat losses to both sides. The stagnation-point boundary layer governing equations for the gas phase (assumed to be frozen) are the following:

$$\frac{\partial(\rho u)}{\partial x} + \frac{\partial(\rho v)}{\partial y} = 0 \tag{1}$$

$$\rho u \frac{\partial u}{\partial x} + \rho v \frac{\partial u}{\partial y} = \frac{\partial}{\partial y}\left(\mu \frac{\partial u}{\partial y}\right) + \rho_\infty a^2 x \tag{2}$$

$$\rho u c_p \frac{\partial T}{\partial x} + \rho v c_p \frac{\partial T}{\partial y} = \frac{\partial}{\partial y}\left(\lambda \frac{\partial T}{\partial y}\right) \tag{3}$$

$$\rho u \frac{\partial \overline{Y}_i}{\partial x} + \rho v \frac{\partial \overline{Y}_i}{\partial y} = \frac{\partial}{\partial y}\left(\rho D_i \frac{\partial \overline{Y}_i}{\partial y}\right) \tag{4}$$

for $i = CH_4$, O_2, and the reaction products. Here u and v are the longitudinal and transversal components of velocity, respectively. The density, viscosity, specific heat at constant pressure, and thermal conductivity of the gas-phase mixture are represented by ρ, μ, c_p, and λ. D_i corresponds to the diffusion coefficient of species i. The associated boundary conditions are the following

$$u = v = \frac{\partial \overline{Y}_{CH_4}}{\partial y} - \frac{\omega W_{CH_4}}{\rho D_{CH_4}} = \frac{\partial \overline{Y}_{O_2}}{\partial y} - \frac{\omega W_{O_2}\sigma}{\rho D_{O_2}}$$

$$= \frac{\partial T}{\partial y} + \frac{\omega Q}{\lambda} - \frac{\lambda_w (T_w - T_\infty)}{\lambda h} = 0 \quad \text{at} \quad y = 0 \tag{5}$$

$$u - ax = T - T_\infty = \overline{Y}_i - \overline{Y}_{i\infty} = 0 \quad \text{for} \quad y \to \infty. \tag{6}$$

Here W_i is the molecular weight of species i; σ is the stoichiometric ratio of the oxidizer related to the fuel of the overall surface reaction, $\sigma = 2$; Q is the heat released by the surface reaction per unit mol of fuel consumed, considering the global reaction $CH_4 + 2O_2 \rightarrow CO_2 + 2H_2O$; λ_w is the thermal conductivity of the plate material; ω is the surface reaction rate given in units of mol of fuel consumed by unit time unit surface of the plate; and T_w corresponds to the temperature at the catalyst surface facing the combustible gaseous mixture.

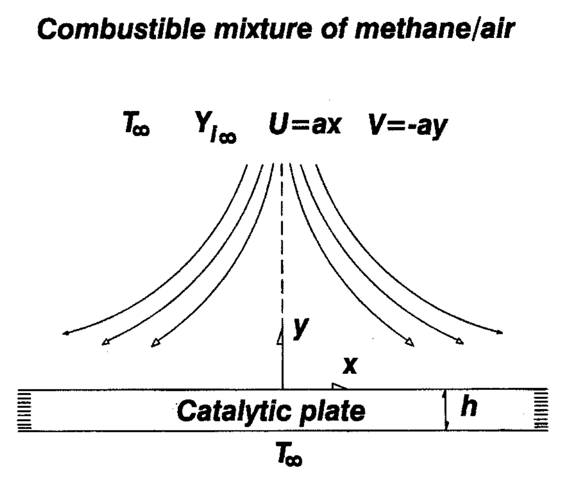

Figure 1. Physical model, showing the adopted flow configuration.

Heterogeneous reaction model

We consider a reaction model to describe the catalytic reactions of the fuel CH_4 and the oxidizer O_2. The model is represented by the heterogeneous reaction mechanism shown in Table 1 (Deutschmann et al., 1996). This mechanism does not contain the adsorption–desorption of intermediate products like CO and H_2, as well the adsorption of H_2O. This is justified for ignition because the concentrations of all these species are extremely low. However, in the diffusion-controlled combustion (ignited branch), these reactions have to be considered, especially the adsorption of water vapor.

The reactions finishing with a and d represent adsorption and desorption, respectively. Here $Pt(s)$ denotes a free site on the surface of the platinum catalyst. All surface reactions are assumed to be of the Langmuir–Hinshelwood type. The adsorption kinetics is given by a sticking probability, S_j, or accommodation coefficient, that represents the portion of the collisions with the surface that successfully leads to adsorption. The rate of collisions, Z_w, can be computed using the classic kinetic theory, with $Z_w = p/\sqrt{2\pi mkT}$, where p and m are the partial pressure and the mass of the involved

Table 1. Heterogeneous Reaction Model

No.	Reaction	S	A	E
1*a*	$CH_4 + 2Pt(s) \rightarrow CH_3(s) + H(s)$	0.01	—	—
2	$CH_3(s) + Pt(s) \rightarrow CH_2(s) + H(s)$	—	3.7×10^{21}	20.0
3	$CH_2(s) + Pt(s) \rightarrow CH(s) + H(s)$	—	3.7×10^{21}	20.0
4	$CH(s) + Pt(s) \rightarrow C(s) + H(s)$	—	3.7×10^{21}	20.0
5	$C(s) + O(s) \rightarrow CO(s) + Pt(s)$	—	3.7×10^{21}	62.8
6	$CO(s) + O(s) \rightarrow CO_2(s) + Pt(s)$	—	3.7×10^{21}	105.0
7*d*	$CO_2(s) \rightarrow CO_2 + Pt(s)$	—	1×10^{13}	20.5
8*a*	$O_2 + 2Pt \rightarrow 2O(s)$	$0.07(300/T)$	—	—
8*d*	$2O(s) \rightarrow O_2 + 2Pt(s)$	—	3.7×10^{21}	$213.2 - 60\theta_O$
9	$H(s) + O(s) \rightarrow OH(s) + Pt(s)$	—	3.7×10^{21}	11.5
10	$H(s) + OH(s) \rightarrow H_2O(s) + Pt(s)$	—	3.7×10^{21}	17.4
11	$OH(s) + OH(s) \rightarrow H_2O(s) + O(s)$	—	3.7×10^{21}	48.2
12*d*	$H_2O(s) \rightarrow H_2O + Pt(s)$	—	1×10^{13}	40.3

Units: **A** (mol·c·s), **E** (kJ/mol).

species, and k is the Boltzmann constant, $k = 1.38 \times 10^{23}$ J/K. On the other hand, the desorption kinetics is well represented by an Arrhenius law with a high activation energy for the important adsorbed species. The adsorbed species concentrations can be represented by the surface coverage θ_i defined by the number of sites occupied by surface species i to the total number of available sites. For the adsorbed species, the steady-state governing equations are then given by

$$\frac{d\theta_{\mathrm{CH}_3}}{dt} = k_{1a}\theta_{\mathrm{V}}^2 - k_2\theta_{\mathrm{CH}_3}\theta_{\mathrm{V}} = 0 \tag{7}$$

$$\frac{d\theta_{\mathrm{CH}_2}}{dt} = k_2\theta_{\mathrm{CH}_3}\theta_{\mathrm{V}} - k_3\theta_{\mathrm{CH}_2}\theta_{\mathrm{V}} = 0 \tag{8}$$

$$\frac{d\theta_{\mathrm{CH}}}{dt} = k_3\theta_{\mathrm{CH}_2}\theta_{\mathrm{V}} - k_4\theta_{\mathrm{CH}}\theta_{\mathrm{V}} = 0 \tag{9}$$

$$\frac{d\theta_{\mathrm{C}}}{dt} = k_4\theta_{\mathrm{CH}}\theta_{\mathrm{V}} - k_5\theta_{\mathrm{C}}\theta_{\mathrm{O}} = 0 \tag{10}$$

$$\frac{d\theta_{\mathrm{CO}}}{dt} = k_5\theta_{\mathrm{C}}\theta_{\mathrm{O}} - k_6\theta_{\mathrm{CO}}\theta_{\mathrm{O}} = 0 \tag{11}$$

$$\frac{d\theta_{\mathrm{CO}_2}}{dt} = k_6\theta_{\mathrm{CO}}\theta_{\mathrm{O}} - k_{7d}\theta_{\mathrm{CO}_2} = 0 \tag{12}$$

$$\begin{aligned}\frac{d\theta_{\mathrm{O}}}{dt} = {} & 2k_{8a}\theta_{\mathrm{V}}^2 - k_5\theta_{\mathrm{C}}\theta_{\mathrm{O}} - k_6\theta_{\mathrm{CO}}\theta_{\mathrm{O}} \\ & - k_9\theta_{\mathrm{H}}\theta_{\mathrm{O}} + k_{11}\theta_{\mathrm{OH}}^2 - 2k_{8d}\theta_{\mathrm{O}}^2 = 0\end{aligned} \tag{13}$$

$$\frac{d\theta_{\mathrm{H}}}{dt} = 4k_{1a}\theta_{\mathrm{V}}^2 - k_9\theta_{\mathrm{H}}\theta_{\mathrm{O}} - k_{10}\theta_{\mathrm{H}}\theta_{\mathrm{OH}} = 0 \tag{14}$$

$$\frac{d\theta_{\mathrm{OH}}}{dt} = k_9\theta_{\mathrm{H}}\theta_{\mathrm{O}} - k_{10}\theta_{\mathrm{H}}\theta_{\mathrm{OH}} - 2k_{11}\theta_{\mathrm{OH}}^2 = 0 \tag{15}$$

$$\frac{d\theta_{\mathrm{H}_2\mathrm{O}}}{dt} = k_{10}\theta_{\mathrm{H}}\theta_{\mathrm{OH}} + k_{11}\theta_{\mathrm{OH}}^2 - k_{12d}\theta_{\mathrm{H}_2\mathrm{O}} = 0 \tag{16}$$

$$\begin{aligned}\theta_{\mathrm{CH}_3} + \theta_{\mathrm{CH}_2} + \theta_{\mathrm{CH}} + \theta_{\mathrm{C}} + \theta_{\mathrm{CO}} + \theta_{\mathrm{CO}_2} \\ + \theta_{\mathrm{O}} + \theta_{\mathrm{H}} + \theta_{\mathrm{OH}} + \theta_{\mathrm{H}_2\mathrm{O}} + \theta_{\mathrm{V}} = 1.\end{aligned} \tag{17}$$

Here θ_{V} denotes the surface coverage of empty or vacant sites. All the reaction rates in Eqs. 7 to 17 are in 1/s units. In this sense, the reaction rates given in Table 1 can be transformed to the appropriate units by

$$k_{1a} = \frac{S_{\mathrm{CH}_4} p\overline{Y}_{\mathrm{CH}_4 w} W}{\Gamma W_{\mathrm{CH}_4}^{3/2}\sqrt{2\pi RT}}, \qquad k_{8a} = \frac{S_{\mathrm{O}_2} p\overline{Y}_{\mathrm{O}_2 w} W}{\Gamma W_{\mathrm{O}_2}^{3/2}\sqrt{2\pi RT}} \tag{18}$$

$$k_r = A_r \exp(-E_r/RT) \quad \text{for} \quad r = 7d, 12d \tag{19}$$

$$k_r = \Gamma A_r \exp(-E_r/RT) \quad \text{for} \quad r = 2,3,4,5,6,8d,9,10,11, \tag{20}$$

where Γ is the surface molar concentration in mol/cm^2, and corresponds to the surface site density ($\sim 10^{15}$ sites/cm^2) divided by the Avogadro number, $Av = 6.02283 \cdot 10^{23}$ molecules/mol. $\Gamma \simeq 1.6603 \cdot 10^{-9}$ mol/cm^2; R is the universal gas constant; and W and W_i are the molecular weight of the mixture and species i, respectively. The reactant concentrations $\overline{Y}_{\mathrm{CH}_4 w}$ and $\overline{Y}_{\mathrm{O}_2 w}$ are the concentrations close to the catalytic surface and are to be obtained after solving the coupled gas-phase equations with the governing equations for the surface coverage of the adsorbed species. We can see that the sticking coefficients of both reactants are very different, in such a way that the most efficient adsorbed species, O(s), almost covers the whole catalytic surface at low temperatures (below the ignition conditions). The sticking probability of the molecular nitrogen N_2 is extremely low, and thus its influence on the surface reactions can be neglected. At low temperatures, the sticking probability of molecular oxygen is large compared with that of the methane, making the surface coverage of adsorbed atomic oxygen very close to unity, $\theta_{\mathrm{O}} \to 1$. From Eqs. 7 to 17 we find that the surface coverage of all the following species are related to θ_{V}, θ_{OH}, and θ_{O} as well as the temperature, as

$$\begin{gathered}\theta_{\mathrm{CH}_3} = \frac{k_{1a}}{k_2}\theta_{\mathrm{V}}, \qquad \theta_{\mathrm{CH}_2} = \frac{k_{1a}}{k_3}\theta_{\mathrm{V}}, \\ \theta_{\mathrm{CH}} = \frac{k_{1a}}{k_4}\theta_{\mathrm{V}}, \qquad \theta_{\mathrm{C}} = \frac{k_{1a}}{k_5}\frac{\theta_{\mathrm{V}}^2}{\theta_{\mathrm{O}}}\end{gathered} \tag{21}$$

$$\theta_{\mathrm{CO}} = \frac{k_{1a}}{k_6}\frac{\theta_{\mathrm{V}}^2}{\theta_{\mathrm{O}}}, \qquad \theta_{\mathrm{CO}_2} = \frac{k_{1a}}{k_{7d}}\theta_{\mathrm{V}}, \qquad \theta_{\mathrm{H}} = \frac{4k_{1a}\theta_{\mathrm{V}}^2}{k_9\theta_{\mathrm{O}} + k_{10}\theta_{\mathrm{OH}}}. \tag{22}$$

Therefore, the steady-state heterogeneous governing equations reduce to

$$\frac{d\theta_{\mathrm{O}}}{dt} = 2k_{8a}\theta_{\mathrm{V}}^2 - 4k_{1a}\theta_{\mathrm{V}}^2 - 2k_{8d}\theta_{\mathrm{O}}^2 = 0 \tag{23}$$

$$\frac{d\theta_{\mathrm{OH}}}{dt} = 2k_{1a}\theta_{\mathrm{V}}^2 - k_{10}\frac{4k_{1a}\theta_{\mathrm{V}}^2\theta_{\mathrm{OH}}}{k_9\theta_{\mathrm{O}} + k_{10}\theta_{\mathrm{OH}}} - k_{11}\theta_{\mathrm{OH}}^2 = 0 \tag{24}$$

$$\frac{d\theta_{\mathrm{H}_2\mathrm{O}}}{dt} = k_{10}\frac{4k_{1a}\theta_{\mathrm{V}}^2\theta_{\mathrm{OH}}}{k_9\theta_{\mathrm{O}} + k_{10}\theta_{\mathrm{OH}}} + k_{11}\theta_{\mathrm{OH}}^2 - k_{12d}\theta_{\mathrm{H}_2\mathrm{O}} = 0, \tag{25}$$

together with Eq. 17, for the four unknowns θ_{O}, θ_{OH}, $\theta_{\mathrm{H}_2\mathrm{O}}$, and θ_{V}.

Gas-Phase Nondimensional Governing Equations

For the gas phase, a stream function $\psi(x, y)$ is introduced to satisfy the mass-conservation equation (Eq. 1): $\rho u = \partial\psi/\partial y$ and $\rho v = -\partial\psi/\partial x$. We also define the following nondimensional variables

$$\begin{gathered}f = \frac{\psi}{x\sqrt{\rho_\infty \mu_\infty a}}, \qquad \eta = \sqrt{\frac{a}{\rho_\infty \mu_\infty}}\int_0^y \rho(x, y')\,dy', \\ \Phi = \frac{c_p W_{\mathrm{CH}_4}(T - T_\infty)}{Q}, \qquad Y_{\mathrm{CH}_4} = \overline{Y}_{\mathrm{CH}_4}, \qquad Y_{\mathrm{O}_2} = \frac{W_{\mathrm{CH}_4}}{\sigma W_{\mathrm{O}_2}}\overline{Y}_{\mathrm{O}_2}.\end{gathered} \tag{26}$$

The resulting nondimensional governing equations now take the form

$$\frac{d^3f}{d\eta^3} + f\frac{d^2f}{d\eta^2} + \frac{\rho_\infty}{\rho} - \left(\frac{df}{d\eta}\right)^2 = 0 \qquad (27)$$

$$\frac{d^2Y_i}{d\eta^2} + fSc_i\frac{dY_i}{d\eta} = \frac{d^2\Phi}{d\eta^2} + fPr\frac{d\Phi}{d\eta} = 0, \qquad (28)$$

where Pr is the Prandtl number of the gaseous mixture, $Pr = \mu c_P/\lambda$, and Sc_i are the Schmidt numbers of the species, $Sc_i = \mu/\rho D_i$. The nondimensional boundary conditions are then given by

$$f = \frac{df}{d\eta} = \frac{dY_i}{d\eta} - GLe_i = \frac{d\Phi}{d\eta} + G - \gamma\Phi_w = 0 \quad \text{at} \quad \eta = 0 \qquad (29)$$

$$\frac{df}{d\eta} - 1 = \Phi = Y_i - Y_{i\infty} = 0 \quad \text{for} \quad \eta \to \infty, \qquad (30)$$

where

$$Le_i = \frac{Sc_i}{Pr}, \quad \gamma = \frac{\lambda_w}{\lambda}\sqrt{\frac{\mu_\infty}{\rho_\infty a h^2}} \quad \text{and} \quad G = \frac{W_{CH_4}Pr\omega}{\sqrt{\rho_\infty \mu_\infty a}}, \qquad (31)$$

where γ is the heat-loss parameter and must be very small compared with unity. The reaction rate ω, which can be obtained from Eqs. 7 to 12, is given by

$$\omega = k_{1a}\theta_V^2\Gamma. \qquad (32)$$

Asymptotic Solution

From Eq. 23 we obtain the relationship between θ_V and θ_O as

$$\theta_V^2 = K_8\theta_O^2, \qquad (33)$$

where $K_8 = k_{8d}/(k_{8a} - 2k_{1a})$ is a function mainly of the temperature. Figure 2 shows the values of the heterogeneous reaction rates k_j as a function of the inverse of the temperature 1,000/T, for a stoichiometric mixture of methane and air. The rates of the desorption reactions for both important products CO_2(s) (k_{7d}) and H_2O(s) (k_{12d}) are very high, indicating the relative low concentrations of both products. The slowest rate at all corresponds to the desorption reaction of the absorbed atomic oxygen, k_{8d}. This rate plays an essential role in determining the ignition condition. The adsorption rate of the molecular oxygen is at least one order of magnitude larger than the adsorption rate of methane, showing that the adsorbed oxygen atoms almost cover the catalytic surface for temperatures below the ignition temperature. Figure 3 shows the evolution of the surface coverage of the surface species as a function of temperature, after solving the set of equations, Eqs. 7 to 17, by assuming that the reactant consumption is negligible, that is, $\overline{Y}_{iw} = \overline{Y}_{i\infty}$. The surface coverages of O(s) is almost unity for temperatures $T \leq 800$ K. For higher temperatures, the desorption process of O(s) is now important, increasing the possibility of adsorbing the fuel species needed for the surface reactions. Surface coverages of O and V are the most important, neglecting all other contributions to Eq. 17, that is, $\theta_O + \theta_V \simeq 1$. Therefore, for values of $\theta_O \sim 1$, $\theta_V \sim \sqrt{K_8}$. Figure 4 shows the reaction rates of the three surface reactions, Eqs. 9–11, where the radical OH(s) plays an important role. Equation 9 is extremely fast, thus reducing drastically the surface coverage of atomic hydrogen, making Eq. 10 very slow compared with Eq. 11. Therefore, we get an excellent approximation by neglecting Eq. 10 compared with the other two, since the adsorbed H_2O(s) is produced mainly by Eq. 11. In this case, θ_H can be approximated by

$$\theta_H \sim \frac{4k_{1a}}{k_9}K_8. \qquad (34)$$

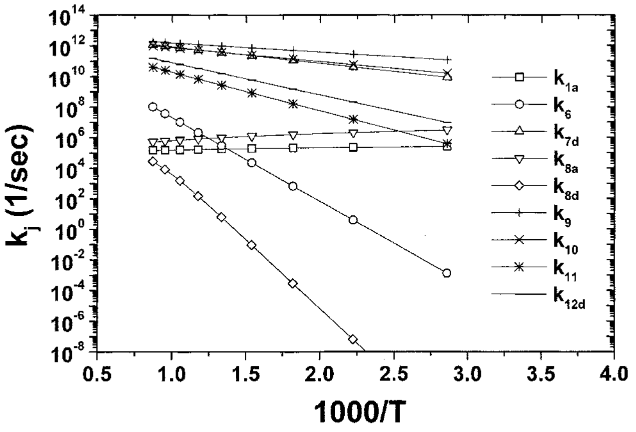

Figure 2. Rates of the most important heterogeneous reactions as a function of the temperature: all the rates are given in s^{-1}.

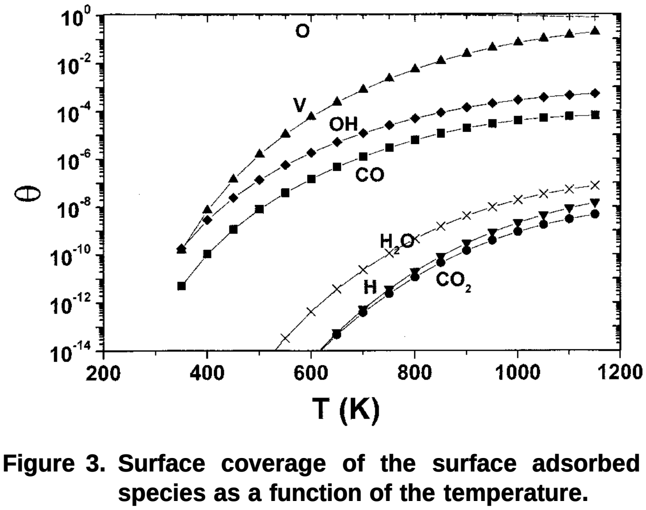

Figure 3. Surface coverage of the surface adsorbed species as a function of the temperature.

Reactant consumption is assumed negligible for this calculation. This behavior is valid for temperatures below the ignition temperature.

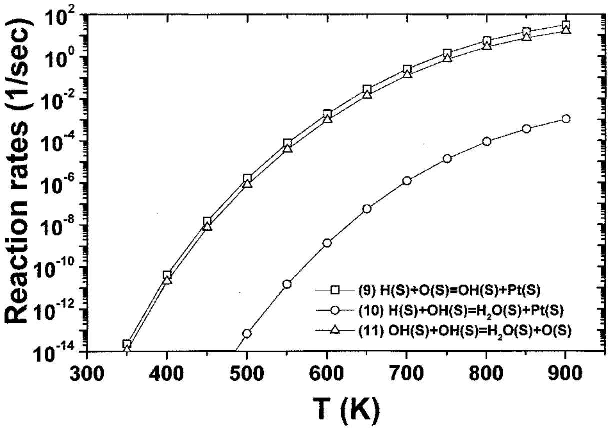

Figure 4. Reaction rates of the surface reactions involving the adsorbed species OH(s).

Reaction 10, given in the figure, is extremely slow and can be neglected when obtaining the critical conditions for ignition.

The chemical reaction is then governed by the adsorption of the fuel as well the adsorption–desorption kinetics of oxygen. From Eq. 33 we obtain a quadratic equation for θ_V as

$$\theta_V^2 + \frac{2K_8}{1-K_8}\theta_V - \frac{K_8}{1-K_8} = 0, \tag{35}$$

with the solution

$$\theta_V = \sqrt{K_8} - K_8 + O\left(K_8^{3/2}\right) \tag{36}$$

$$\theta_O = 1 - \sqrt{K_8} + K_8 + O\left(K_8^{3/2}\right), \quad \text{for} \quad K_8 \to 0. \tag{37}$$

The reaction rate can be approximated well by

$$\omega = k_{1a}\theta_V^2\Gamma \simeq \Gamma k_{1a}K_8, \tag{38}$$

where we use the leading-order term in θ_V^2, neglecting the terms of order $K_8^{3/2}$. Due to the fact that k_{8d} has a large activation energy (desorption of O(s)), the surface reaction rate is strongly dependent on temperature. The surface chemical reaction produces vacant sites that are rapidly occupied by fresh adsorbed species. Additional free sites are obtained when the newly generated adsorbed product of the surface reaction is rapidly desorbed. The surface reaction is exothermic, thus increasing the temperature and therefore increasing the desorption of O(s). This process finally leads to a thermal runaway, which characterizes the catalytic ignition process. In Eq. 38, it is shown that the reaction rate depends on the adsorption kinetics of both reactants and in the desorption kinetics of oxygen, which depends strongly on temperature. To generate the ignition conditions, it is enough to consider a temperature increase due to the heterogeneous reactions of the order $T_w - T_\infty \sim RT_\infty/E_{8d}$. It is then convenient to define a new variable of order unity for the nondimensional temperature as

$$\varphi = \frac{E_{8d}Q}{c_p W_{CH_4} R T_\infty^2}\Phi \sim 1. \tag{39}$$

With this new variable, the nondimensional governing equations take the form

$$\frac{d^3f}{d\eta^3} + f\frac{d^2f}{d\eta^2} + 1 + \epsilon\varphi - \left(\frac{df}{d\eta}\right)^2 = 0 \tag{40}$$

$$\frac{d^2y_i}{d\eta^2} + fSc_i\frac{dy_i}{d\eta} = \frac{d^2\varphi}{d\eta^2} + fPr\frac{d\varphi}{d\eta} = 0, \tag{41}$$

with the boundary conditions

$$f = \frac{df}{d\eta} = \frac{dy_i}{d\eta} - \Delta\exp(\varphi_w)$$

$$= \frac{d\varphi}{d\eta} + \Delta\exp(\varphi_w) - \gamma\varphi_w = 0 \quad \text{at} \quad \eta = 0 \tag{42}$$

$$\frac{df}{d\eta} - 1 = \varphi = y_i - y_{i\infty} = 0 \quad \text{for} \quad \eta \to \infty, \tag{43}$$

where

$$y_i = \frac{Y_i}{\epsilon Le_i}\frac{Q}{c_p W_{CH_4} T_\infty} \quad \text{and}$$

$$\Delta = \frac{Q}{\epsilon c_p T_\infty}\frac{Pr}{\sqrt{\rho_\infty \mu_\infty a}}k_{1a}\Gamma K_{8\infty}, \tag{44}$$

where $K_{8\infty}$ is K_8 computed with $T = T_\infty$. For large activation energy of the desorption reaction for the fuel, $\epsilon = RT_\infty/(E_{8d}) \to 0$, the temperature variation close to the ignition condition is very small, and thus in a first approximation both adsorption reactions can be assumed to be temperature independent. The Damköhler number for the surface reactions is expressed as Δ. In the limit $\epsilon \to 0$, the solution to Eqs. 40 to 43 can be found elsewhere (Treviño, 1983):

$$\left.\frac{dy_i}{d\eta}\right|_{\eta=0} = 0.57Sc_i^{2/5}(y_{i\infty} - y_{iw}) = \Delta\exp(\varphi_w) \tag{45}$$

$$\left.\frac{d\varphi}{d\eta}\right|_{\eta=0} = -0.57Pr^{2/5}\varphi_w = -\Delta\exp(\varphi_w) + \gamma\varphi_w. \tag{46}$$

The first equation takes into account reactant consumption. From Eq. 46 we can obtain the critical conditions for catalytic ignition as

$$\Delta_I = \frac{0.57Pr^{2/5}(1+\bar{\gamma})}{\exp(1)}$$

where

$$\bar{\gamma} = \frac{\gamma}{0.57Pr^{2/5}}. \tag{47}$$

From Eq. 45, the reactants' concentration at the wall, at ignition conditions, is given by

$$Y_{iw} = Y_{i\infty} - \frac{\epsilon Le_i^{3/5} c_p W_{CH_4} T_\infty}{Q}(1+\bar{\gamma}). \tag{48}$$

In general, for practical purposes, reactant consumption can be neglected in obtaining the critical conditions for igniting the catalyst. The mass diffusion in the boundary layer is then important after reaching ignition conditions. In the ignited branch, the strong surface reactions are diffusion limited.

Conclusions

The ignition condition given by Eq. 47, with the definition of the Damköhler number given in Eq. 44, represents parametric dependence on the catalytic ignition. The ignition process depends on the adsorption kinetics of both reactants and the desorption kinetics of oxygen. The Damköhler number for ignition is then given by

$$\Delta_I = \frac{Q}{c_p T_\infty} \frac{E_{8d}}{RT_\infty} \frac{Pr}{\sqrt{\rho_\infty \mu_\infty a}} \frac{\Gamma^2 A_{8d} \exp\left[-\frac{E_{8d}}{RT_\infty}\right]}{\left(\frac{S_{O_2}\overline{Y}_{O_2 w} W_{CH_4}^{3/2}}{S_{CH_4}\overline{Y}_{CH_4 w} W_{O_2}^{3/2}} - 2\right)}$$

$$= \frac{0.57 Pr^{2/5}(1+\overline{\gamma})}{\exp(1)}. \qquad (49)$$

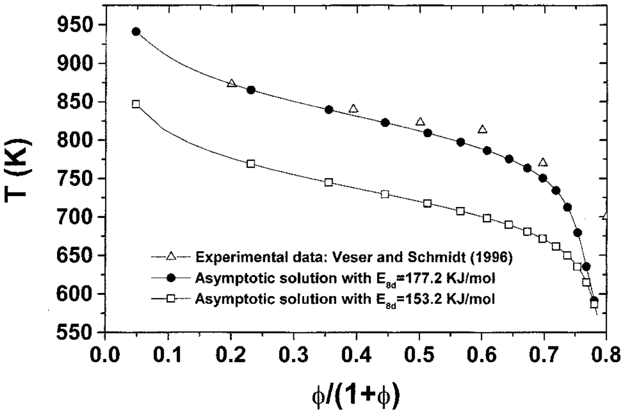

Figure 5. Ignition temperature of the mixture of methane and air over a platinum foil in a stagnation-point flow as a function of the mixture equivalence ratio $\phi/(1+\phi)$.

The asymptotic results are given for a velocity gradient $a = 20\ s^{-1}$. The open rectangles correspond to a surface coverage of O(s) of unity in computing the activation energy of the desorption reaction $8d$. The solid circles correspond to an activation energy of the desorption reaction $8d$ of $E_{8d} = 177.2$ kJ/mol. The triangles correspond to the experimental results reported by Veser and Schmidt (1996).

The ignition temperature can be obtained from the transcendental Eq. 49. Due to the fact that in general the activation energy of the desorption reaction is very large, the ignition temperature has a weak logarithmic dependence on the physical flow parameters. In order to obtain the ignition temperature, we must give the value for the activation energy of the desorption of O(s), $E_{8d} = 213.2 - 60\theta_O$. This means that the surface coverage of O(s) has to be obtained at the ignition conditions, $\theta_O = 1 - K_{8\infty}^{1/2}$. Figure 5 shows the ignition temperature of a mixture of methane and air as a function of fuel concentration $\phi/(1+\phi)$. Here ϕ denotes the fuel-to-air mass ratio related to the stoichiometric value, so $\phi = 1$ (or $\phi/(1+\phi) = 0.5$) then indicates the stoichiometric mixture. For this case, we used a velocity gradient of $a = 20\ s^{-1}$. For comparison, the experimental results by Veser and Schmidt (1996), represented by triangles, are also shown. The experimental conditions reported by these authors are very different from those assumed in this work. Veser and Schmidt used an externally heated catalytic foil, where the mixture temperature corresponds to the room temperature. In the present article, the mixture temperature corresponds to the ignition temperature, without any external power supply. Establishment of a relationship between the ignition temperatures using these two different experimental conditions is left for future work. However, using both experimental configurations, the trends have to be similar. The curve denoted by open rectangles corresponds to the case where the activation energy of the desorption reaction $8d$ is assumed with a surface coverage of O(s) of unity, that is $E_{8d} = 213.2 - 60 = 153.2$ kJ/mol. Using this value, the asymptotic solution underestimates the ignition temperature by 100 K. However, when we try an activation energy of the desorption reaction of $E_{8d} = 177.2$ kJ/mol, the asymptotic solution plotted with solid circles shows very good agreement with the experimental results, except for very rich mixtures. Because of the very high value of the activation energy involved, the asymptotic solution reflects closely the numerical solution of the governing equations. The ignition temperature is highly dependent on the activation energy of reaction $8d$ and the ratio of the adsorption rates of both reactants

$$\frac{S_{O_2}\overline{Y}_{O_2 w} W_{CH_4}^{3/2}}{S_{CH_4}\overline{Y}_{CH_4 w} W_{O_2}^{3/2}}. \qquad (50)$$

This ratio is close to 10 for a stoichiometric mixture, and so its influence is weak. As the mixtures becomes richer, the adsorption rate of the fuel increases, reducing this ratio, and thus reducing the ignition temperature. For values of ϕ of order 4, this ratio becomes very close to 2, and then the denominator of Eq. 49 rapidly decreases, which also decreases the ignition temperature. In this condition, however, the surface coverage of O(s) stops being close to unity, which means that the main assumption used to develop the asymptotic solution is not fulfilled anymore resulting in the breakdown of the solution. Theoretically, for extremely rich mixtures, the adsorption rate of methane becomes more important, which would cause the direction of the ignition temperature with ϕ to reverse.

Acknowledgments

This work was supported by the Hungarian Academy of Sciences (MTA) and CONACyT, Mexico. I thank T. Turanyi of the Eötvos Lorand University of Budapest, for his valuable comments and observations on this work.

Literature Cited

Behrendt, F., O. Deutschmann, R. Schmidt, and J. Warnatz, "Investigation of Ignition and Extinction of Hydrogen-Air and Methane-Air Mixtures over Platinum and Palladium," Symposium on Catalysis, Heterogeneous Hydrocarbon Oxidation, ACS, New Orleans, LA (1996).

Bui, P.-A., D. G. Vlachos, and P. R. Westmoreland, "Homogeneous Ignition of Hydrogen-Air Mixtures over Platinum," *Proc. Symp. (Int.) on Combustion*, The Combustion Institute, Pittsburgh, PA, p. 1,763 (1996).

Bui, P.-A., D. G. Vlachos, and P. R. Westmoreland, "Modeling Ignition of Catalytic Reactors with Detailed Surface Kinetics and Transport: Oxidation of H_2/O_2 Mixtures over Platinum Surfaces," *Ind. Eng. Chem. Res.*, **36**, 2,558 (1997a).

Bui, P.-A., D. G. Vlachos, and P. R. Westmoreland, "Catalytic Ignition of Methane/Oxygen Mixtures over Platinum Surfaces: Comparison of Detailed Simulations and Experiments," *Surf. Sci.*, **385**, L1029 (1997b).

Bui, P.-A., D. G. Vlachos, and P. R. Westmoreland, "Hierarchial Reduced Models for Catalytic Combustion: H_2/Air Mixtures Near Platinum Surfaces," *Combust. Sci. Technol.*, **129**(1/6), 243 (1997c).

Deutschmann, O., R. Schmidt, F. Behrendt, and J. Warnatz, "Numerical Modeling of Catalytic Ignition," *Proc. Symp. (Int.) on Combustion*, The Combustion Institute, Pittsburgh, PA, p. 1747 (1996).

Ertl, G., "Chemical Dynamics in Surface Reactions," *Ber. Bunsenges. Phys. Chem.*, **86**, 425 (1982).

Fassihi, M., V. P. Zhdanov, M. Rinnemo, K.-E. Keck, and B. Kasemo, "A Theoretical and Experimental Study of Catalytic Ignition in the Hydrogen-Oxygen Reaction on Platinum," *J. Catal.*, **141**, 438 (1993).

Ljungström, S., B. Kasemo, A. Rosen, T. Wahnström, and E. Fridell, *Surf. Sci.*, **216**, 63 (1989).

Pfefferle, L. D., and W. C. Pfefferle, "Catalysis in Combustion," *Catal. Res. Sci. Eng.*, **29** (2&3), 219 (1987).

Rinnemo, M., M. Fassihi, and B. Kasemo, "The Critical Condition for Catalytic Ignition. H_2/O_2 on Pt," *Chem. Phys. Lett.*, **211**, 60 (1993).

Song, X., W. R. Williams, L. D. Schmidt, and R. Aris, "Ignition and Extinction of Homogeneous-Heterogeneous Combustion: CH_4 and C_3H_8 Oxidation on Pt," *Proc. Symp. (Int.) on Combustion*, The Combustion Institute, Pittsburgh, PA, p. 1129 (1990).

Treviño, C., "Gas-Phase Ignition of Premixed Fuel by Catalytic Bodies in Stagnation Flow," *Combust. Sci. Technol.*, **30**, 213 (1983).

Treviño, C., "An Asymptotic Analysis of the Catalytic Ignition in a Stagnation-Point Flow," *Combust. Theory Modelling* (1998).

Treviño, C., and A. C. Fernández-Pello, "Catalytic Flat Plate Boundary Layer Ignition," *Combust. Sci. Technol.*, **26**, 245 (1981).

Treviño, C., and N. Peters, "Gas-Phase Boundary Layer Ignition on a Catalytic Flat Plate with Heat Loss," *Combust. Flame*, **61**, 39 (1985).

Treviño, C., and F. Méndez, "Ignition of Catalytic Reactions in a Vertical Plate Immersed in a Combustible Gas," *Proc. Symp. (Int.) on Combustion*, The Combustion Institute, Pittsburgh, PA, p. 1,797 (1996).

Veser, G., and L. D. Schmidt, "Ignition and Extinction in the Catalytic Oxidation of Hydrocarbons over Platinum," *AIChE J.*, **42**, 1077 (1996).

Warnatz, J., "Resolution of Gas-Phase and Surface Combustion Chemistry into Elementary Reactions," *Proc. Symp. (Int.) on Combustion*, The Combustion Institute, Pittsburgh, PA, p. 553 (1992).

Warnatz, J., M. D. Allendorf, R. J. Kee, and M. Coltrin, "A Model of Elementary Chemistry and Fluid Mechanics in the Combustion of Hydrogen on Platinum Surfaces," *Combust. Flame*, **96**, 393 (1994).

Williams, W. R., M. T. Stenzel, X. Song, and L. D. Schmidt, "Bifurcation Behavior in Homogeneous-Heterogeneous Combustion: 1. Experimental Results over Platinum," *Combust. Flame*, **84**, 277 (1991).

Williams, W. R., C. M. Marks, and L. D. Schmidt, "Steps in the Reaction $H_2 + O_2 \rightleftharpoons H_2O$ on Pt: OH Desorption at High Temperatures," *J. Phys. Chem.*, **96**, 5922 (1992).

Manuscript received Sept. 2, 1998, and revision received Dec. 5, 1998.